

Nonstructural Protein $\sigma 1s$ Mediates Reovirus-Induced Cell Cycle Arrest and Apoptosis

Karl W. Boehme,^{a,b} Katharina Hammer,^{c,d*} William C. Tollefson,^{c,d*} Jennifer L. Konopka-Anstadt,^{c,d} Takeshi Kobayashi,^{c,d*} Terence S. Dermody^{c,d,e}

Department of Microbiology and Immunology^a and Center for Microbial Pathogenesis and Host Inflammatory Response,^b University of Arkansas for Medical Sciences, Little Rock, Arkansas, USA; Departments of Pediatrics^c and Pathology, Microbiology, and Immunology^e and Elizabeth B. Lamb Center for Pediatric Research,^d Vanderbilt University School of Medicine, Nashville, Tennessee, USA

Reovirus nonstructural protein $\sigma 1s$ is implicated in cell cycle arrest at the G₂/M boundary and induction of apoptosis. However, the contribution of $\sigma 1s$ to these effects in an otherwise isogenic viral background has not been defined. To evaluate the role of $\sigma 1s$ in cell cycle arrest and apoptosis, we used reverse genetics to generate a $\sigma 1s$ -null reovirus. Following infection with wild-type virus, we observed an increase in the percentage of cells in G₂/M, whereas the proportion of cells in G₂/M following infection with the $\sigma 1s$ -null mutant was unaffected. Similarly, we found that the wild-type virus induced substantially greater levels of apoptosis than the $\sigma 1s$ -null mutant. These data indicate that $\sigma 1s$ is required for both reovirus-induced cell cycle arrest and apoptosis. To define sequences in $\sigma 1s$ that mediate these effects, we engineered viruses encoding C-terminal $\sigma 1s$ truncations by introducing stop codons in the $\sigma 1s$ open reading frame. We also generated viruses in which charged residues near the $\sigma 1s$ amino terminus were replaced individually or as a cluster with nonpolar residues. Analysis of these mutants revealed that amino acids 1 to 59 and the amino-terminal basic cluster are required for induction of both cell cycle arrest and apoptosis. Remarkably, viruses that fail to induce cell cycle arrest and apoptosis also are attenuated *in vivo*. Thus, identical sequences in $\sigma 1s$ are required for reovirus-induced cell cycle arrest, apoptosis, and pathogenesis. Collectively, these findings provide evidence that the $\sigma 1s$ -mediated properties are genetically linked and suggest that these effects are mechanistically related.

Apoptosis is a critical host response to viral infection. Induction of apoptotic cell death limits production of viral progeny from infected cells (1) and provides signals that activate adaptive immune responses (2–4). Although thought to be initiated as a protective measure for the host, apoptosis also causes the pathology associated with many viral diseases. Defining viral and cellular determinants that govern virus-induced apoptosis is of fundamental importance to an understanding of viral pathogenesis.

Mammalian orthoreoviruses (reoviruses) are highly tractable models for studies of viral replication and pathogenesis (5). Reoviruses are nonenveloped, icosahedral viruses with segmented double-stranded RNA (dsRNA) genomes. The different reovirus serotypes display differences in cell tropism (6, 7), mechanism of viral dissemination (8), apoptosis induction (9), and central nervous system (CNS) disease (5). In newborn mice, serotype 3 (T3) reoviruses infect neurons and cause apoptosis that leads to lethal encephalitis (8, 10–12). T3 reoviruses also induce high levels of apoptosis in cultured cells (13). Serotype 1 (T1) reoviruses infect ependymal cells and cause ependymitis and hydrocephalus (11, 12). However, T1 reoviruses induce markedly less apoptosis than T3 reoviruses in cell culture (13). Differences in apoptosis induction segregate with the viral S1 gene segment (9), which encodes attachment protein $\sigma 1$ and nonstructural protein $\sigma 1s$ (14–17), and the M2 gene segment (9, 18), which encodes outer-capsid protein $\mu 1$ (14, 15). Fragments of the $\mu 1$ protein generated during virus entry activate intrinsic apoptotic pathways (19–23). However, it is not known how attachment protein $\sigma 1$ or nonstructural protein $\sigma 1s$ contributes to reovirus apoptosis.

Protein $\sigma 1s$ is a 14-kDa nonstructural protein encoded by the viral S1 gene segment (16, 24, 25). The $\sigma 1s$ open reading frame (ORF) completely overlaps the $\sigma 1$ coding sequence; however, $\sigma 1s$ lies in a different reading frame (16, 24–27). Little amino acid

sequence identity exists in the $\sigma 1s$ proteins from different reovirus serotypes (24, 27). The only feature of the $\sigma 1s$ protein that is conserved across the serotypes is a cluster of positively charged amino acids near the amino terminus (24, 27). For T3 reovirus, this cluster is hypothesized to function as a nuclear localization signal (28).

The $\sigma 1s$ protein has been implicated in reovirus-induced cell cycle arrest at the G₂/M boundary (29, 30) and may function in reovirus neurovirulence by influencing apoptosis in the murine CNS (31). However, interpreting these studies of $\sigma 1s$ function is complicated because the $\sigma 1s$ -null mutant virus used in previous experiments is not isogenic to the parental strain from which it was derived (32). Serial passage of a T3 field isolate strain, T3C84, in cell culture yielded a variant, T3C84-MA, which due to introduction of a premature stop codon after the seventh amino acid in the $\sigma 1s$ ORF does not express $\sigma 1s$ (32). Following infection with T3C84, the percentage of cells in the G₂/M phase of the cell cycle is increased compared to that after mock infection. In contrast, after

Received 26 July 2013 Accepted 17 September 2013

Published ahead of print 25 September 2013

Address correspondence to Karl W. Boehme, kwboehme@uams.edu.

* Present address: Katharina Hammer, University Group Oncolytic Adenoviruses, German Cancer Research Center, Heidelberg University Hospital, Heidelberg, Germany; William C. Tollefson, Department of Geography and Anthropology, Howe-Russell Geoscience Complex, Louisiana State University, Baton Rouge, Louisiana, USA; Takeshi Kobayashi, Laboratory of Viral Replication, International Research Center for Infectious Diseases, Research Institute for Microbial Diseases, Osaka University, Suita, Osaka, Japan.

Copyright © 2013, American Society for Microbiology. All Rights Reserved.

doi:10.1128/JVI.02080-13

infection with T3C84-MA, the percentage of cells in G₂/M is similar to that of uninfected controls (30). Although these results suggest a role for σ 1s in reovirus-induced cell cycle arrest, the viruses used for these studies are not isogenic. Unlike the parental virus, T3C84-MA harbors, in addition to the mutation affecting σ 1s expression, a second mutation in the S1 gene that confers binding of σ 1 to cell surface sialic acid (33). Importantly, the capacity to bind sialic acid enhances reovirus-induced apoptosis (34) and virulence *in vivo* (35). Moreover, there may be additional mutations in T3C84-MA acquired during serial passage that influence these phenotypes. Using σ 1s-deficient viruses generated by reverse genetics, we found that T1 and T3 reoviruses require σ 1s to disseminate within an infected host using hematogenous pathways (36, 37). However, the mechanism by which σ 1s promotes spread via the blood is not known.

In this study, we used wild-type and σ 1s-null T3 reoviruses generated by reverse genetics to determine whether σ 1s is required for reovirus-induced cell cycle arrest and apoptosis; these viruses are isogenic except for σ 1s expression. We found that the σ 1s-null mutant failed to cause cell cycle arrest and induced lower levels of apoptosis than the wild-type virus. Using a panel of mutant viruses, we identified σ 1s residues 1 to 59 and a cluster of basic amino acids near the amino terminus as essential for both effects. Mutants defective for cell cycle arrest and apoptosis also are attenuated *in vivo*. Collectively, these findings suggest that cell cycle arrest, apoptosis, and reovirus virulence are mechanistically linked.

MATERIALS AND METHODS

Cell lines. L929 cells were maintained in Joklik's minimal essential medium (SMEM; Lonza) supplemented to contain 5% fetal bovine serum (FBS), 2 mM L-glutamine, 100 U/ml penicillin, 100 μ g/ml streptomycin, and 25 ng/ml amphotericin B. HeLa cells were maintained in Dulbecco's MEM (DMEM; Gibco) supplemented to contain 10% FBS, 2 mM L-glutamine, 100 U/ml penicillin, 100 μ g/ml streptomycin, and 25 ng/ml amphotericin B (Invitrogen). HCT-116 cells were maintained in McCoy's 5a medium (Gibco) supplemented to contain 10% FBS, 2 mM L-glutamine, 100 U/ml penicillin, 100 μ g/ml streptomycin, and 25 ng/ml amphotericin B (Invitrogen).

Preparation of murine cortical neuron cultures. Primary cultures of mouse cortical neurons were established using cerebral cortices of C57/BL6 embryos at embryonic day 15 (E15) (38). Fetuses were decapitated, their brains were removed, and their cortical lobes were dissected and submerged in Hanks' balanced salt solution (Gibco) on ice. Cortices were incubated in 0.6 mg/ml trypsin solution at room temperature for 30 min, washed twice, and manually dissociated twice with a Pasteur pipette. Viable cells were plated at a density of 2.75×10^5 cells/ml in 24-well plates (Corning) or on glass coverslips (BD Biosciences) placed in 24-well plates. Wells were treated prior to plating with a 10- μ g/ml poly-D-lysine solution (BD Biosciences) and a 1.64- μ g/ml laminin solution (BD Biosciences). Cultures were incubated for the first 24 h in neurobasal medium (Gibco) supplemented to contain 10% FBS (Gibco), 0.6 mM L-glutamine, 50 U/ml penicillin, and 50 μ g/ml streptomycin. Cultures were thereafter maintained in neurobasal medium supplemented to contain $1 \times B27$ (Gibco), 50 units/ml penicillin, and 50 μ g/ml streptomycin. One-half of the medium was replaced every 3 to 4 days. Neurons were allowed to mature for 7 days prior to use.

Viruses. Recombinant reoviruses were generated using plasmid-based reverse genetics (39). Monolayers of L929 cells at approximately 90% confluence (3×10^6 cells) in 60-mm dishes (Corning) were infected with rDIs-T7 pol at a multiplicity of infection (MOI) of ~ 0.5 50% tissue culture infective dose (TCID₅₀)/cell. At 1 h postinfection, cells were cotransfected with 9 plasmid constructs representing cloned gene segments from

the strain type 3 Dearing (T3D) genome—pT7-L1T3D (2 μ g), pT7-L2T3D (2 μ g), pT7-L3T3D (2 μ g), pT7-M1T3D (1.75 μ g), pT7-M2T3D (1.75 μ g), pT7-M3T3D (1.75 μ g), pT7-S2T3D (1.5 μ g), pT7-S3T3D (1.5 μ g), and pT7-S4T3D (1.5 μ g)—in combination with 2 μ g of pBacT7-S1T3D, pBacT7-S1T3D σ 1s-null, pBacT7-S1T3D σ 1s-S41Stop, pBacT7-S1T3D σ 1s-L60Stop, pBacT7-S1T3D σ 1s-L80Stop, pBacT7-S1T3D σ 1s-L97stop, pBacT7-S1T3D σ 1s-R14L, pBacT7-S1T3D σ 1s-R14L/R15L, or pBacT7-S1T3D σ 1s-R14L/R15L/R19L. For each transfection, 3 μ l of TransIT-LT1 transfection reagent (Mirus) was used per μ g of plasmid DNA. Following 5 days of incubation, recombinant virus was isolated from transfected cells by plaque purification using monolayers of L929 cells (40). For generation of σ 1s mutant viruses, pBacT7-S1T3D was altered by QuikChange (Stratagene) site-directed mutagenesis. Sequences of mutant viruses were confirmed using S1 gene cDNAs prepared from viral RNA extracted from purified virions subjected to OneStep reverse transcriptase PCR (RT-PCR) (Qiagen) with S1-specific primers. Changes introduced into the σ 1s ORF did not alter the σ 1 protein sequence. Primer sequences are available from the corresponding author upon request. PCR products were analyzed following electrophoresis in Tris-borate-EDTA agarose gels or purified and subjected directly to sequence analysis. The presence of a noncoding signature mutation in the L1 gene of viruses generated by plasmid-based rescue was confirmed using RT-PCR and L1-specific primers (39).

Purified reovirus virions were generated using second- or third-passage L929 cell lysate stocks of twice-plaque-purified reovirus as described previously (41). Viral particles were Freon extracted from infected cell lysates, layered onto 1.2- to 1.4-g/cm³ CsCl gradients, and centrifuged at $62,000 \times g$ for 18 h. Bands corresponding to virions (1.36 g/cm³) (42) were collected and dialyzed in virion storage buffer (150 mM NaCl, 15 mM MgCl₂, 10 mM Tris-HCl [pH 7.4]). The concentration of reovirus virions in purified preparations was determined from an equivalence to one optical density (OD) unit at 260 nm (2.1×10^{12} virions) (42). Viral titer was determined by plaque assay using L929 cells (40).

Virus replication assays. L929 cells (5×10^4 cells/well) seeded in 24-well plates were adsorbed in triplicate with reovirus strains at an MOI of 1 PFU/cell at room temperature for 1 h in serum-free medium, washed once with phosphate-buffered saline (PBS), and incubated in serum-containing medium for various intervals. Cells were frozen and thawed twice prior to determination of viral titer by plaque assay using L929 cells (40).

Flow cytometry. L929 cells (10^6 cells/well) seeded in 6-well plates were adsorbed with reovirus strains at various MOIs at room temperature for 1 h. At various intervals postinfection, cells were trypsinized, transferred to microcentrifuge tubes, washed twice with PBS, and fixed in 70% ethanol at 4°C overnight. Cells were washed twice with PBS and stained with Krishan's stain, containing 3.8 mM trisodium citrate (Sigma), 70 μ M propidium iodide (Sigma), 0.01% Nonidet P-40 (Sigma), and 0.01 mg of RNase A (Boehringer Mannheim) per ml (43). Cellular DNA content was quantified using a Coulter Epics XL flow cytometer (Beckman-Coulter). Alignment of the instrument was verified daily using DNA check beads (Coulter). Peak versus integral gating was used to exclude doublet events from the analysis. Data were collected for 10,000 events. Cell cycle modeling was accomplished using the Flow-Jo program (Verity Software House).

Quantification of apoptosis by AO staining. L929, HeLa, or HCT-116 cells (5×10^4 cells/well) seeded in 24-well plates were adsorbed with reovirus strains at various MOIs at room temperature for 1 h. After 48 h of incubation, the percentage of apoptotic cells was determined using acridine orange (AO) staining as described previously (13). For each experiment, >200 cells were counted, and the percentage of cells exhibiting condensed chromatin was determined by epi-illumination fluorescence microscopy using a fluorescein filter set (Zeiss).

Assessment of caspase 3/7 activity. HeLa cells (2×10^5 cells/well) seeded in 24-well plates were adsorbed with reovirus strains at an MOI of 100 PFU/cell at room temperature for 1 h. Cells were frozen 24 h postinfection, and caspase 3/7 activity in thawed lysates containing 5×10^3 cell

equivalents was quantified using the Caspase-Glo-3/7 assay system (Promega) according to the manufacturer's instructions.

Assessment of reovirus infectivity by indirect immunofluorescence. Monolayers of L929, HeLa, or HCT-116 cells (2×10^5 cells/well) seeded in 24-well plates were adsorbed with reovirus strains at an MOI of 1 PFU/cell at room temperature for 1 h. Inocula were removed, cells were washed once with PBS, and fresh medium was added. Cells were incubated at 37°C for 24 h, washed once with PBS, and fixed with ice-cold methanol for 30 min at 4°C. Cells were washed twice with PBS prior to being blocked with 5% bovine serum albumin (BSA) in PBS at room temperature for 15 min. Cells were incubated with polyclonal reovirus-specific serum diluted 1:500 in PBS containing 0.5% Triton X-100 at room temperature for 1 h. Primary antibody was removed, and cells were washed twice with PBS and incubated with 4',6-diamidino-2-phenylindole (DAPI; Invitrogen) and Alexa Fluor 488-labeled goat anti-rabbit fluorescent secondary antibody (Invitrogen), both diluted 1:1,000 in PBS containing 0.5% Triton X-100, at room temperature for 1 h. Cells were washed twice with PBS, and infected cells were visualized by fluorescence microscopy. Results are expressed as the mean percentage of infected cells present in three $\times 10$ -magnification fields of view.

Assessment of $\sigma 1s$ expression by confocal microscopy. Monolayers of HeLa cells (10^5 cells/well) grown on coverslips in 24-well plates were adsorbed with reovirus at an MOI of 10 PFU/cell at room temperature for 1 h. Following removal of the inoculum, cells were washed with PBS and incubated in complete medium at 37°C for 18 h to permit completion of a single cycle of viral replication. Monolayers were fixed with 1 ml of methanol at 20°C for at least 30 min, washed twice with PBS, and blocked with 0.1% gelatin, 0.1% Tween 20 (Sigma), and 20% normal goat serum (Vector Laboratories) in PBS. For detection of $\sigma 1s$, cells were washed with PBS and incubated with mouse monoclonal anti- $\sigma 1s$ antibody 2F4 (44) at a dilution of 1:500 in PBS with 0.1% gelatin, 2% normal goat serum, and 0.1% Tween 20. For detection of reovirus proteins, cells were washed once with PBS and stained with polyclonal rabbit antireovirus serum at a 1:1,000 dilution in PBS–0.5% Triton X-100 at room temperature for 1 h. Monolayers were washed twice with PBS–0.5% Triton X-100 and incubated with a 1:1,000 dilution of Alexa 488- or Alexa 546-labeled anti-rabbit or anti-mouse IgG (Invitrogen), respectively. Monolayers were washed with PBS, and infected cells were visualized by confocal microscopy using a Ti-U microscope with a $60\times/1.4$ -numerical-aperture (NA) oil immersion objective (Nikon). Images were analyzed using NIS-Elements software (Nikon) and normalized for pixel intensity, brightness, and contrast.

Infection of mice. C57BL/6J mice were obtained from Jackson Laboratory. Newborn mice weighing 1.5 to 2 g were inoculated intramuscularly with purified reovirus diluted in PBS. Intramuscular inoculations (10 μ l) were delivered into the left hind limb using a Hamilton syringe and 30-gauge needle. Mice were monitored for weight loss and symptoms of disease for 21 days postinoculation and euthanized when found to be moribund (defined by rapid or shallow breathing, lethargy, or paralysis). Death was not used as an endpoint in these experiments. Animal husbandry and experimental procedures were performed in accordance with Public Health Service policy and approved by the Vanderbilt University School of Medicine Institutional Animal Care and Use Committee.

Statistical analysis. Means of results from triplicate samples were compared using an unpaired Student *t* test. Differences in viral virulence were determined using a log-rank test. Statistical analyses were performed using Prism software (GraphPad Software, Inc.). *P* values of <0.05 were considered to be statistically significant.

RESULTS

The $\sigma 1s$ protein is required for reovirus-induced cell cycle arrest. To determine whether $\sigma 1s$ is required for reovirus-induced cell cycle arrest, L929 cells were mock infected or infected with rsT3D or rsT3D $\sigma 1s$ -null at an MOI of 100 PFU/cell. At 24 h postinfection, cellular DNA was stained with propidium iodide

and quantified by flow cytometry (Fig. 1A). We observed a >2 -fold increase in the percentage of cells with 4N DNA content (representing cells in G_2 or mitosis) following infection with rsT3D relative to that in mock-infected cells. In contrast, rsT3D $\sigma 1s$ -null did not alter the proportion of cells in the G_2 and M phases of the cell cycle. Infection of HeLa cells (Fig. 1B) or HCT116 cells (Fig. 1C) with rsT3D $\sigma 1s$ -null also did not alter the percentage of cells in G_2 /M. To ensure that differences in the capacities of rsT3D and rsT3D $\sigma 1s$ -null to induce cell cycle arrest do not reflect a difference in infectivity between the two viruses, we quantified the number of infected cells 24 h after inoculation of L929, HeLa, and HCT-116 cells. No difference in infectivity of rsT3D and rsT3D $\sigma 1s$ -null was observed in any of the cell lines tested (Fig. 1D). This result is consistent with our previous finding that rsT3D and rsT3D $\sigma 1s$ -null produce comparable yields of viral progeny in cultured cells (36). Thus, failure of rsT3D $\sigma 1s$ -null to induce cell cycle arrest is not attributable to a defect in infectivity or replication. These results indicate that $\sigma 1s$ is required for reovirus-induced cell cycle arrest.

The $\sigma 1s$ protein is required for reovirus-induced apoptosis. To determine whether $\sigma 1s$ is required for reovirus-induced apoptosis, L929 cells were mock infected or infected with rsT3D or rsT3D $\sigma 1s$ -null at an MOI of 100 PFU/cell. Apoptotic nuclei were quantified by AO staining at 48 h postinfection (Fig. 2A). We found that rsT3D induced apoptosis in nearly 100% of cells. Although rsT3D $\sigma 1s$ -null induced more apoptosis than was observed in mock-infected cells, the level of apoptosis was substantially lower than that following infection with rsT3D. Even when the infectious dose of rsT3D $\sigma 1s$ -null was 10-fold higher than a dose of rsT3D that elicits apoptosis in nearly 100% of cells (1,000 PFU/cell for rsT3D $\sigma 1s$ -null versus 100 PFU/cell for rsT3D), the capacity of rsT3D $\sigma 1s$ -null to induce apoptosis was reduced (Fig. 2E). Concordantly, rsT3D $\sigma 1s$ -null also induced less caspase 3/7 activity than rsT3D (Fig. 2F). These findings are not restricted to cell type, as rsT3D $\sigma 1s$ -null elicited lower levels of apoptosis than rsT3D in HeLa cells (Fig. 2B), HCT116 cells (Fig. 2C), and primary cultures of murine cortical neurons (Fig. 2D). Together, these findings indicate that $\sigma 1s$ expression significantly potentiates the capacity of reovirus to induce apoptotic cell death.

Cell cycle arrest precedes apoptosis following reovirus infection. To define the kinetics of cell cycle arrest and apoptosis during reovirus infection, L929 cells were mock infected or infected with rsT3D at an MOI of 100 PFU/cell. Cell cycle status was assessed (Fig. 3A), and apoptotic cells were quantified (Fig. 3B) at 12-h intervals over a 48-h period. Cell cycle progression was not affected by rsT3D until 24 h postinfection. At this time point, the percentage of cells with a 4N DNA content was approximately twice that detected following mock infection. Although no differences in the percentages of cells in G_2 /M were detected between mock- and rsT3D-infected cells at 36 or 48 h postinfection, cell cycle modeling at those times is imprecise due to cytopathic effects associated with late stages of viral infection. Apoptosis was not detected in rsT3D-infected cells until 36 h postinfection, and levels of apoptosis were increased at 48 h. These data indicate that cell cycle arrest occurs prior to the induction of apoptosis during reovirus infection.

Identical sequences in $\sigma 1s$ mediate cell cycle arrest and apoptosis. To define sequences in $\sigma 1s$ required for cell cycle arrest and apoptosis, we used reverse genetics to generate reoviruses expressing truncated $\sigma 1s$ proteins. Stop codons were inserted into

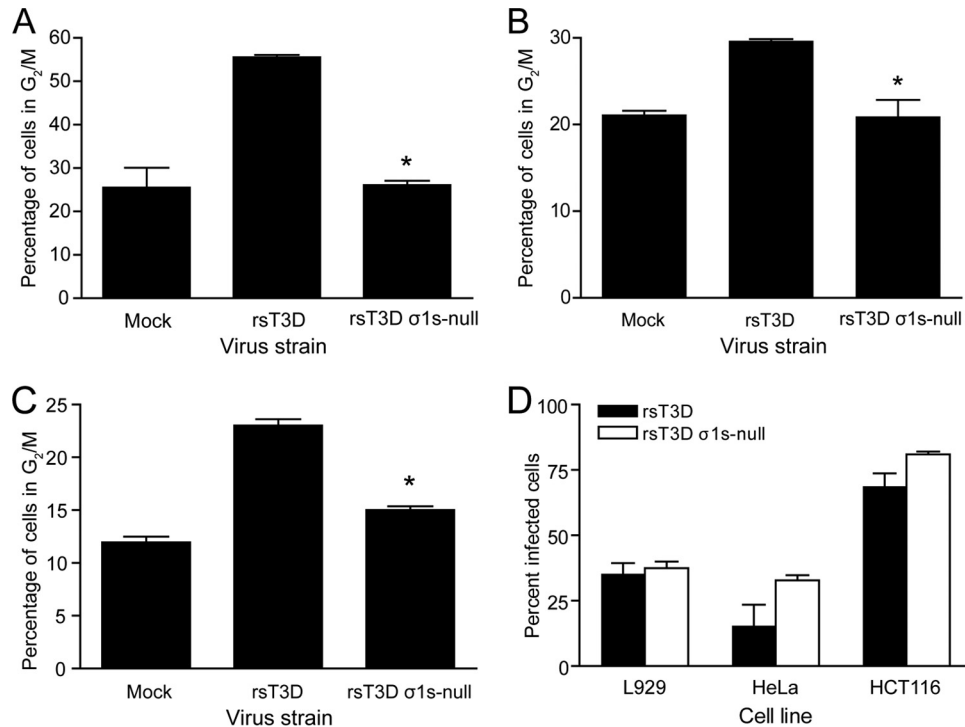


FIG 1 The σ 1s protein is required for reovirus-induced cell cycle arrest. (A to C) L929 (A), HeLa (B), or HCT-116 (C) cells were mock infected or infected with rsT3D or rsT3D σ 1s-null at an MOI of 100 PFU/cell. At 24 h postinfection, cells were stained with propidium iodide, and cellular DNA content was quantified by flow cytometry. Results are expressed as the mean percentage of cells with a 4N DNA content, which represents cells in the G₂ or M phases of the cell cycle, for three independent experiments. (D) L929, HeLa, or HCT116 cells were inoculated with rsT3D or rsT3D σ 1s-null at an MOI of 1 PFU/cell. At 24 h postinoculation, infected cells were quantified by indirect immunofluorescence. Results are expressed as the mean percentage of infected cells in a $\times 10$ -magnification field of view for three independent samples. Error bars indicate standard deviations (SD). *, $P < 0.05$ (determined by Student's t test in a comparison with rsT3D-infected cells).

the σ 1s ORF at amino acid positions 41, 60, 80, and 97 to yield the following viruses: rsT3D σ 1s 1–40, rsT3D σ 1s 1–59, rsT3D σ 1s 1–79, and rsT3D σ 1s 1–96. Stop codon insertion and the absence of other S1 gene mutations were confirmed by direct sequencing of viral RNA (data not shown). To determine whether truncating the σ 1s protein affects reovirus replication in cell culture, we quantified viral yields following infection of L929 cells (Fig. 4A). Yields of infectious progeny for each mutant were equivalent to those produced by rsT3D. Moreover, immunoblot analysis of infected cell lysates revealed no differences in viral protein levels between rsT3D and the truncation mutants (Fig. 4B). These findings indicate that truncating the σ 1s protein does not affect viral gene expression or replication in cultured cells.

To identify sequences in σ 1s required for reovirus-induced cell cycle arrest, L929 cells were mock infected or infected with rsT3D, rsT3D σ 1s-null, or each of the σ 1s truncation mutants at an MOI of 100 PFU/cell. We used L929 cells for cell cycle analysis because experiments using these cells provided the largest dynamic range of the three cell lines tested. At 24 h postinfection, cellular DNA was stained with propidium iodide and quantified by flow cytometry (Fig. 5A). We found that the percentage of cells in G₂/M was increased following infection with rsT3D σ 1s 1–59, rsT3D σ 1s 1–79, and rsT3D σ 1s 1–96 but not to the levels achieved by rsT3D. In contrast, rsT3D σ 1s 1–40 did not alter the percentage of cells in G₂/M relative to mock infection. These findings indicate that amino acids 1 to 59 in σ 1s are required for reovirus-induced cell cycle arrest. Residues 60 to 120 in σ 1s are not essential for this

property, but these sequences may enhance the capacity of the protein to cause cell cycle dysregulation.

To identify sequences in σ 1s required for apoptosis induction, HeLa cells were mock infected or infected with rsT3D, rsT3D σ 1s-null, or each of the σ 1s truncation viruses at an MOI of 100 PFU/cell. In parallel cultures, apoptosis induction was assessed by quantifying caspase 3/7 activity or determining the percentage of apoptotic cells using AO staining (Fig. 5B and C). We assessed apoptosis in HeLa cells because experiments using these cells provided the largest dynamic range of the three cell lines tested. By both measures, rsT3D σ 1s 1–96 induced levels of apoptosis comparable to those elicited by rsT3D. Strikingly, levels of apoptosis were markedly higher following infection with rsT3D σ 1s 1–59 and rsT3D σ 1s 1–79 than with rsT3D. In contrast, rsT3D σ 1s 1–40 induced significantly less apoptosis than did the wild-type virus. These results indicate that σ 1s residues 1 to 59 are required for apoptosis induction and suggest that σ 1s amino acids 60 to 96 function as a regulatory domain that negatively modulates the capacity of σ 1s to promote apoptosis. Together, these findings indicate that the same amino acids in σ 1s are required for reovirus-induced cell cycle arrest and apoptosis induction, suggesting that these properties are mechanistically linked.

The σ 1s amino-terminal basic cluster is required for reovirus-induced cell cycle arrest and apoptosis. To determine whether the σ 1s amino-terminal basic cluster is required for reovirus-induced cell cycle arrest and apoptosis, we used reverse genetics to generate three mutant viruses in which arginine residues

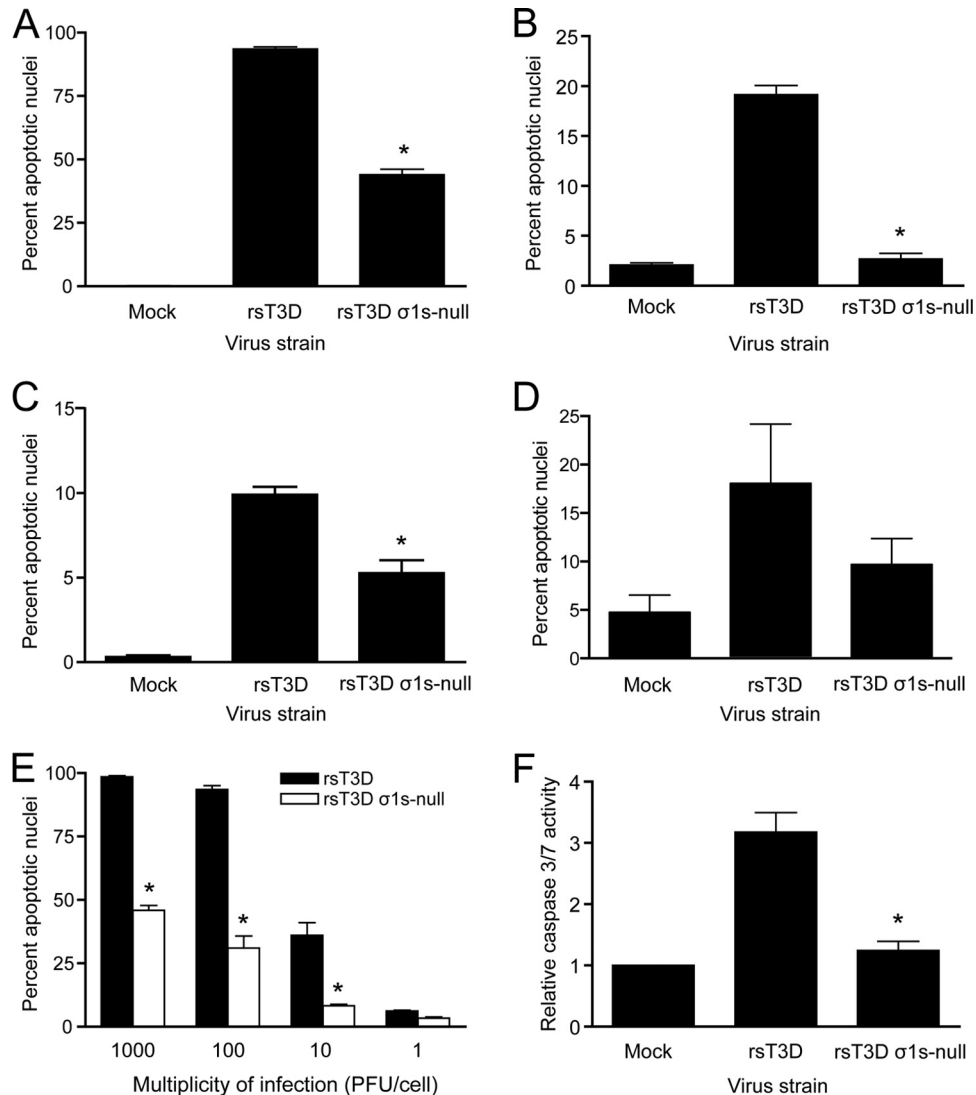


FIG 2 The $\sigma 1s$ protein enhances reovirus-induced apoptosis. (A to D) L929 (A), HeLa (B), or HCT-116 (C) cells or mouse primary cortical neurons (D) were mock infected or infected with rsT3D or rsT3D $\sigma 1s$ -null at an MOI of 100 PFU/cell. At 48 h postinfection, the percentage of apoptotic nuclei was determined following AO staining. (E) L929 cells were infected with rsT3D or rsT3D $\sigma 1s$ -null at the indicated MOIs. At 48 h postinfection, the percentage of apoptotic nuclei was determined following AO staining. Results are expressed as the mean percentage of apoptotic nuclei for three independent experiments. Error bars indicate SD. (F) HeLa cells were mock infected or infected with rsT3D or rsT3D $\sigma 1s$ -null at an MOI of 100 PFU/cell. Caspase 3/7 activity was quantified at 24 h postinfection. Results are expressed as the mean caspase 3/7 activity relative to that in mock-infected cells for three independent experiments. Error bars indicate SD. *, $P < 0.0001$ (determined by Student's t test in a comparison with rsT3D-infected cells).

at positions 14, 15, and 19 in the basic cluster (R¹⁴RSRRRLK²¹) were replaced individually or in combination with leucine to yield the following viruses: rsT3D $\sigma 1s$ R14L, rsT3D $\sigma 1s$ R14L/R15L, and rsT3D $\sigma 1s$ R14L/R15L/R19L. In each case, the arginine-to-leucine substitution preserved the coding sequence of the overlapping $\sigma 1$ ORF. Arginine 17, arginine 18, and lysine 21 cannot be altered without changing the $\sigma 1$ coding sequence. The arginine-to-leucine substitutions and absence of other S1 gene mutations were confirmed by direct sequencing of viral RNA (data not shown). To test whether altering the $\sigma 1s$ basic cluster affects viral replication, we quantified viral yields following infection of L929 cells (Fig. 6A). Yields of infectious progeny for each mutant were equivalent to those produced by rsT3D. This finding indicates that the $\sigma 1s$ basic cluster is not required for reovirus replication in

cultured cells. In addition, no differences in viral protein levels were detected between rsT3D and the $\sigma 1s$ basic cluster mutants, indicating that viral gene expression is not affected by altering the charge in this region of $\sigma 1s$ (Fig. 6B). Thus, basic residues at some positions in the $\sigma 1s$ amino-terminal basic cluster are dispensable for viral gene expression and replication in cultured cells.

To determine whether the $\sigma 1s$ amino-terminal basic cluster is required for reovirus-induced cell cycle arrest, L929 cells were mock infected or infected with rsT3D, rsT3D $\sigma 1s$ -null, rsT3D $\sigma 1s$ R14L, rsT3D $\sigma 1s$ R14L/R15L, or rsT3D $\sigma 1s$ R14L/R15L/R19L at an MOI of 100 PFU/cell. At 24 h postinfection, cellular DNA was stained with propidium iodide and quantified by flow cytometry (Fig. 7A). The percentage of cells in G₂/M was significantly lower following infection with all three basic cluster mutants than with

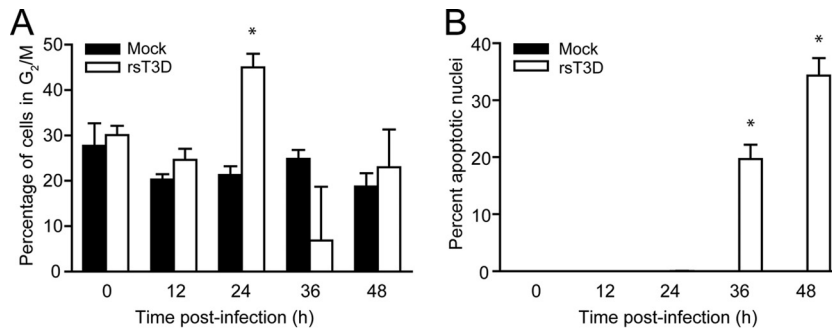


FIG 3 Cell cycle arrest precedes apoptosis during reovirus infection. (A) L929 cells were either mock infected or infected with rsT3D at an MOI of 100 PFU/cell. At the indicated times postinfection, cells were stained with propidium iodide, and cellular DNA content was quantified by flow cytometry. Results are expressed as the mean percentage of cells with a 4N DNA content for three independent experiments. Error bars indicate SD. *, $P < 0.05$ by Student's t test in comparison to mock infection. (B) HeLa cells were either mock infected or infected with rsT3D at an MOI of 100 PFU/cell. At the indicated times postinfection, the percentage of apoptotic nuclei was determined following AO staining. Results are expressed as the mean percentage of apoptotic nuclei from three independent experiments. Error bars indicate SD. *, $P < 0.0001$ (determined by Student's t test in a comparison with mock-infected cells).

rsT3D. These data indicate that the $\sigma 1s$ amino-terminal basic cluster is required for reovirus-induced cell cycle arrest.

To determine whether the $\sigma 1s$ amino-terminal basic cluster is required for apoptosis induction, HeLa cells were mock infected

or infected with rsT3D, rsT3D $\sigma 1s$ -null, rsT3D $\sigma 1s$ R14L, rsT3D $\sigma 1s$ R14L/R15L, or rsT3D $\sigma 1s$ R14L/R15L/R19L at an MOI of 100 PFU/cell. In parallel cultures, apoptosis induction was assessed by quantifying caspase 3/7 activity (Fig. 7B) or determining the percentage of apoptotic cells using AO staining (Fig. 7C). By both techniques, each $\sigma 1s$ basic cluster mutant was impaired in apoptosis induction compared with rsT3D, indicating that the $\sigma 1s$ basic cluster is required for reovirus-induced apoptosis. We conclude that the $\sigma 1s$ amino-terminal basic cluster is an essential sequence region for reovirus-induced cell cycle arrest and apoptosis, which provides further evidence that these effects are linked.

Changes in the amino-terminal basic cluster do not affect $\sigma 1s$ nuclear translocation. To test whether altering the $\sigma 1s$ amino-terminal basic cluster affects the capacity of the protein to enter the nucleus, HeLa cells were mock infected or infected with rsT3D, rsT3D $\sigma 1s$ R14L, rsT3D $\sigma 1s$ R14L/R15L, or rsT3D $\sigma 1s$ R14L/R15L/R19L. At 24 h postinfection, the intracellular distribution of $\sigma 1s$ was assessed by indirect immunofluorescence (Fig. 8). The $\sigma 1s$ protein of wild-type rsT3D was observed in the nucleus and cytoplasm, consistent with results of previous reports (28, 32, 36). The $\sigma 1s$ proteins of all three basic cluster mutant viruses were similarly distributed at the time point tested. These data indicate that mutations in the amino-terminal basic cluster do not alter $\sigma 1s$ nuclear translocation and suggest that the basic cluster is not required for nuclear localization.

Sequences in $\sigma 1s$ essential for cell cycle arrest and apoptosis induction are required for reovirus virulence. To determine whether sequences in $\sigma 1s$ required for cell cycle arrest and apoptosis induction also are required for reovirus virulence, we inoculated newborn C57BL/6 mice in the left hind limb muscle with 10^6 PFU of rsT3D, rsT3D $\sigma 1s$ -null, rsT3D $\sigma 1s$ 1–40, rsT3D $\sigma 1s$ 1–59, or rsT3D $\sigma 1s$ R14L/R15L (Fig. 9). Mice were monitored for 21 days for signs of disease and euthanized when moribund. Hind limb inoculations were performed because reovirus strain T3D replicates poorly in the gastrointestinal tract and fails to disseminate systemically from that site (45–47). All mice inoculated with rsT3D succumbed to infection. The median survival time (MST) for animals infected with rsT3D was 9 days (Table 1). In contrast, 50% of mice survived infection with rsT3D $\sigma 1s$ -null (MST = 18 days). Similarly, 55% of mice survived infection with rsT3D $\sigma 1s$ R14L/R15L, suggesting that the $\sigma 1s$ amino-terminal basic

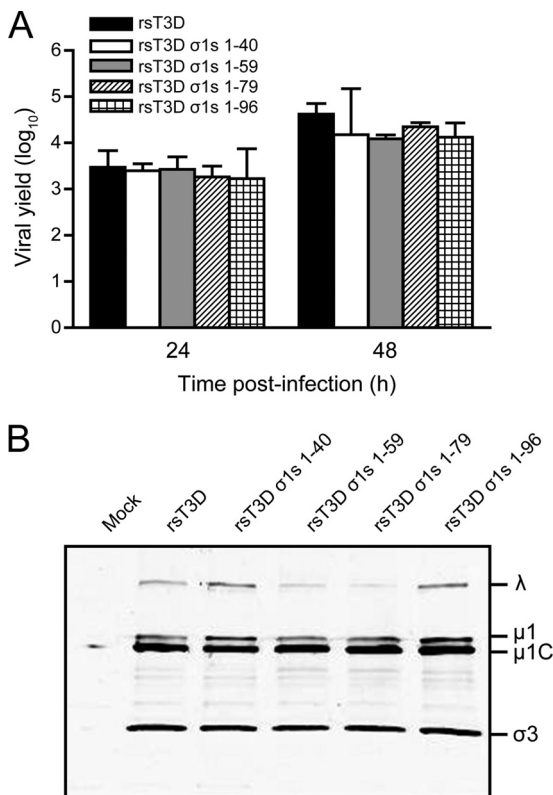


FIG 4 Truncation of the $\sigma 1s$ protein does not alter reovirus replication in cell culture. (A) L929 cells were infected with rsT3D, rsT3D $\sigma 1s$ 1–40, rsT3D $\sigma 1s$ 1–59, rsT3D $\sigma 1s$ 1–79, or rsT3D $\sigma 1s$ 1–96 at an MOI of 1 PFU/cell. Titers of virus in cell lysates were determined by plaque assay at 24 and 48 h postinfection. Results are expressed as the mean viral yield for triplicate samples. Error bars indicate SD. (B) L929 cells were mock infected or infected with rsT3D, rsT3D $\sigma 1s$ 1–40, rsT3D $\sigma 1s$ 1–59, rsT3D $\sigma 1s$ 1–79, or rsT3D $\sigma 1s$ 1–96 at an MOI of 100 PFU/cell. Whole-cell lysates were prepared from infected cells at 48 h postinfection and resolved by SDS-polyacrylamide gel electrophoresis. Reovirus proteins were detected by immunoblotting using a reovirus-specific polyclonal antiserum. Reovirus proteins are labeled on the right.

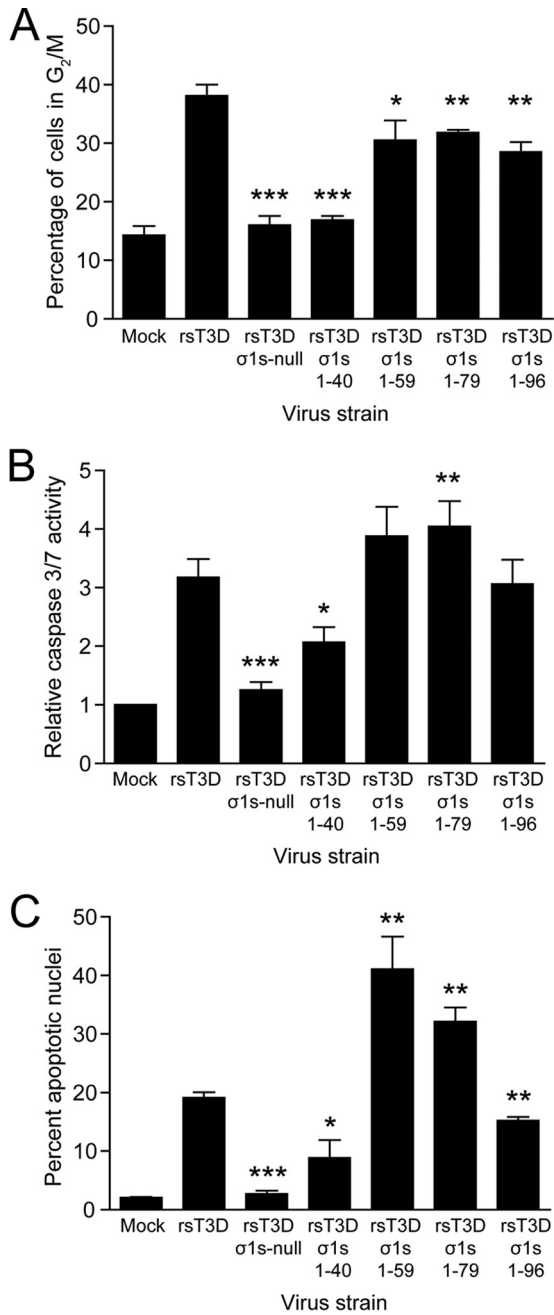


FIG 5 Amino acids 1 to 59 of $\sigma 1s$ are required for reovirus-induced cell cycle arrest and apoptosis. (A) L929 cells were mock infected or infected with rsT3D, rsT3D $\sigma 1s$ -null, rsT3D $\sigma 1s$ 1–40, rsT3D $\sigma 1s$ 1–59, rsT3D $\sigma 1s$ 1–79, or rsT3D $\sigma 1s$ 1–96 at an MOI of 100 PFU/cell. At 24 h postinfection, cells were stained with propidium iodide, and cellular DNA content was quantified by flow cytometry. Results are expressed as the mean percentage of cells with a 4N DNA content from three independent experiments. Error bars indicate SD. *, $P < 0.05$; **, $P < 0.005$; ***, $P < 0.0001$ (as determined by Student's t test in comparison with rsT3D). (B and C) HeLa cells were mock infected or infected with rsT3D, rsT3D $\sigma 1s$ -null, rsT3D $\sigma 1s$ 1–40, rsT3D $\sigma 1s$ 1–59, rsT3D $\sigma 1s$ 1–79, or rsT3D $\sigma 1s$ 1–96 at an MOI of 100 PFU/cell. Caspase 3/7 activity was quantified at 24 h postinfection (B), and the percentages of apoptotic nuclei were determined following AO staining at 48 h postinfection (C). Shown are mean values from three independent experiments. Error bars indicate SD. *, $P < 0.01$; **, $P < 0.005$; ***, $P < 0.0001$ (as determined by Student's t test in a comparison with rsT3D-infected cells).

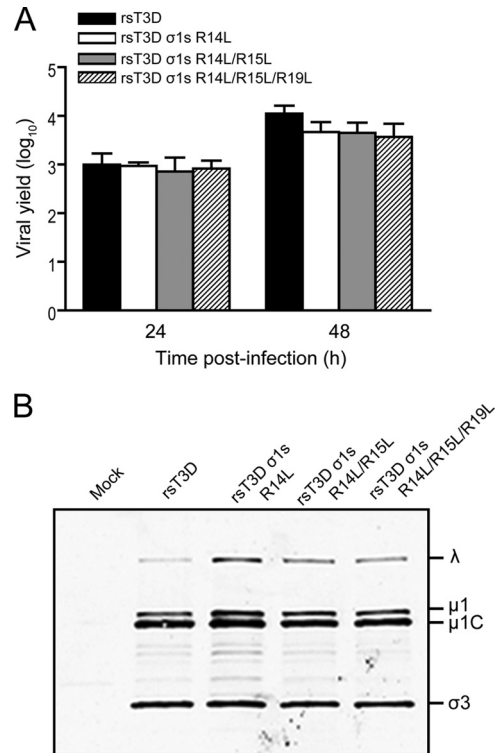


FIG 6 The $\sigma 1s$ N-terminal basic cluster is not required for reovirus replication in cell culture. (A) L929 cells were infected with rsT3D, rsT3D $\sigma 1s$ R14L, rsT3D $\sigma 1s$ R14L/R15L, or rsT3D $\sigma 1s$ R14L/R15L/R19L at an MOI of 1 PFU/cell. Titers of virus in cell lysates were determined by plaque assay at 24 and 48 h postinfection. Results are expressed as the mean viral yields from triplicate samples. Error bars indicate SD. (B) L929 cells were mock infected or infected with rsT3D, rsT3D $\sigma 1s$ R14L, rsT3D $\sigma 1s$ R14L/R15L, or rsT3D $\sigma 1s$ R14L/R15L/R19L at an MOI of 100 PFU/cell. Whole-cell lysates were prepared from infected cells at 48 h postinfection and resolved by SDS-polyacrylamide gel electrophoresis. Reovirus proteins were detected by immunoblotting using a reovirus-specific polyclonal antiserum. Reovirus proteins are labeled on the right.

cluster is required for reovirus virulence. The rsT3D $\sigma 1s$ 1–59 mutant was slightly attenuated compared with rsT3D; 19% of mice survived infection (MST = 12 days). However, the rsT3D $\sigma 1s$ 1–40 mutant was substantially attenuated, with a survival rate of 88%. These results indicate that $\sigma 1s$ residues 1 to 59 are essential for full reovirus virulence. Collectively, these findings indicate that sequences in $\sigma 1s$ required for cell cycle arrest and apoptosis induction also are required for reovirus pathogenesis, which suggests a mechanistic link between cell cycle dysregulation, apoptosis induction, and disease.

DISCUSSION

Nonstructural protein $\sigma 1s$ is required for hematogenous reovirus dissemination (36, 37). However, mechanisms by which $\sigma 1s$ promotes systemic spread have not been determined. Previous studies using a $\sigma 1s$ -deficient reovirus strain suggest that $\sigma 1s$ inhibits cell cycle progression at the G₂/M boundary (29) and influences reovirus-induced apoptosis (31). However, interpreting these studies is complicated by the use of viruses that are not isogenic with respect to $\sigma 1s$ expression. In this study, we used isogenic viruses generated by reverse genetics to determine whether $\sigma 1s$ mediates reovirus cell cycle arrest and apoptosis. We found that

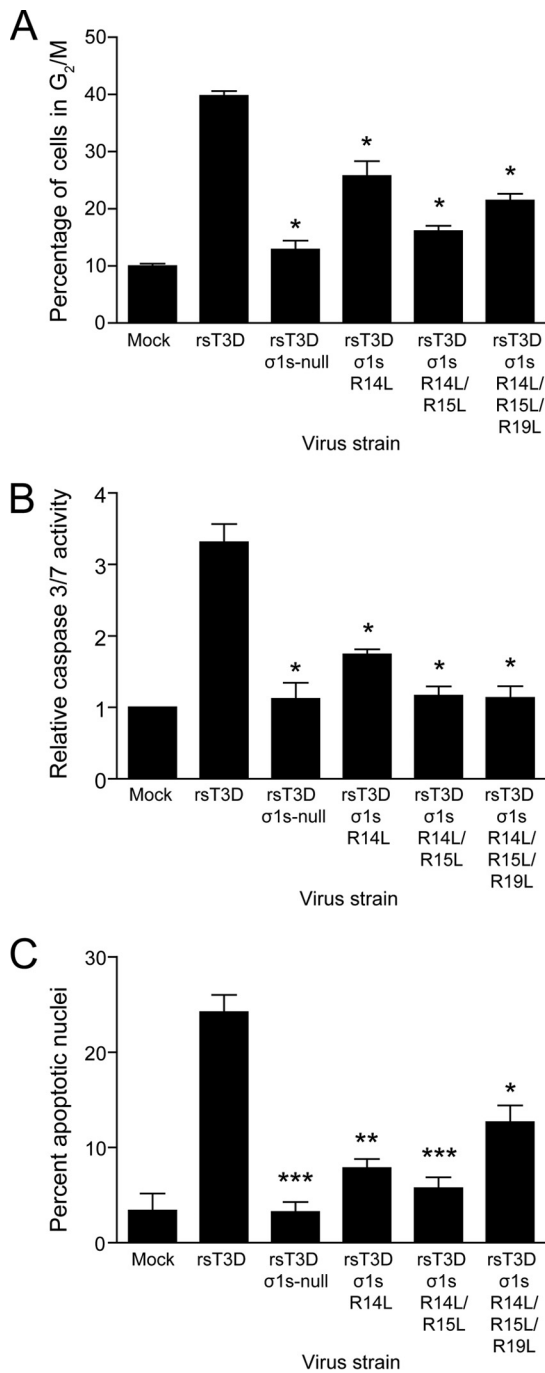


FIG 7 The σ 1s N-terminal basic cluster is required for reovirus-induced cell cycle arrest and apoptosis. (A) L929 cells were mock infected or infected with rsT3D, rsT3D σ 1s-null, rsT3D σ 1s R14L, rsT3D σ 1s R14L/R15L, or rsT3D σ 1s R14L/R15L/R19L at an MOI of 100 PFU/cell. At 24 h postinfection, cells were stained with propidium iodide, and cellular DNA content was quantified by flow cytometry. Results are expressed as the mean percentage of cells with a 4N DNA content from three independent experiments. Error bars indicate SD. *, $P < 0.05$ (as determined by Student's t test in a comparison with rsT3D-infected cells). (B and C) HeLa cells were mock infected or infected with rsT3D, rsT3D σ 1s-null, rsT3D σ 1s R14L, rsT3D σ 1s R14L/R15L, or rsT3D σ 1s R14L/R15L/R19L at an MOI of 1,000 PFU/cell. Caspase 3/7 activity was quantified at 24 h postinfection (B) and the percentage of apoptotic nuclei was determined following AO staining at 48 h postinfection (C). Shown are mean values from three independent experiments. Error bars indicate SD. *, $P < 0.05$; **, $P < 0.005$; ***, $P < 0.001$ (as determined by Student's t test in a comparison with rsT3D-infected cells).

σ 1s expression is required for cell cycle arrest, consistent with previous studies. We also found that σ 1s enhances reovirus-induced apoptosis. Using a panel of mutant viruses, we identified σ 1s amino acids 1 to 59 and the amino-terminal basic cluster as essential for both effects. Finally, we found that mutant viruses that fail to induce cell cycle arrest and apoptosis also are attenuated *in vivo*. Together, these data provide evidence that σ 1s-mediated cell cycle arrest, apoptosis, and virulence are genetically linked and suggest that a common mechanism underlies these effects.

Although our data indicate that σ 1s mediates cell cycle arrest and apoptosis in reovirus-infected cells, it is not known how these effects are functionally associated. During cell division, cell cycle arrest and apoptosis act in concert to prevent passing damaged DNA to daughter cells. If DNA is damaged or replication stress is detected, checkpoints are activated to inhibit cell cycle progression. Repair of such damage terminates the arrest and allows the cell cycle to proceed through mitosis. When the damage cannot be repaired, apoptosis is induced to ensure that daughter cells receive only faithfully replicated DNA. We envision three possibilities to explain how σ 1s-dependent cell cycle arrest leads to apoptosis during reovirus infection. First, σ 1s may trigger cellular pathways that are activated by DNA damage or replication stress. For example, activation of the DNA damage response (DDR) proteins ataxia telangiectasia mutated (ATM) or ATM-Rad3-related (ATR) can induce cell cycle arrest that leads to apoptosis (48). Although activation of ATM and ATR following DNA virus infection is well documented (49), RNA viruses also can activate these pathways. For example, Rift Valley fever virus causes cell cycle arrest in an ATM-dependent manner (50). Avian reovirus induces phosphorylation of ATM that is consistent with DDR activation and causes G₂/M arrest (51). However, it is not known whether DDR induction leads to cell cycle arrest or apoptosis in avian-reovirus-infected cells. Second, σ 1s may halt cell cycle progression by inhibiting cell cycle regulatory proteins. Several viruses encode proteins that cause cell cycle arrest and apoptosis by blocking the activities of cell cycle control factors. Adenovirus E4orf4 (52) and hepatitis B virus X protein (53) directly engage components of the anaphase-promoting complex (APC), which powers mitotic exit. Cell cycle arrest and apoptosis can result from impaired APC function (54). In reovirus-infected cells, σ 1s might inhibit cell cycle progression by interfering with the function of cellular proteins that control the G₂-to-M transition, with the resultant stress associated with prolonged arrest in G₂ leading to apoptosis. Third, σ 1s may indirectly elicit cell cycle arrest and apoptosis by disrupting a vital cellular process that causes cell stress. For example, the σ 1s protein is implicated in altering the architecture of the nuclear envelope by disrupting the lamin network, which is integral to nuclear structure and function (28). Disrupting nuclear lamin can activate the DNA replication checkpoint, leading to cell cycle arrest and ultimately apoptosis (55, 56). Identifying cellular proteins that interact with σ 1s will likely provide insight into how σ 1s functions to cause cell cycle arrest and apoptotic cell death.

If the contribution of σ 1s to reovirus apoptosis is dependent on induction of cell cycle arrest, then the proapoptotic activity of σ 1s would manifest only in actively dividing cells. A causal relationship between σ 1s-dependent cell cycle arrest and apoptosis would explain why rsT3D and rsT3D σ 1s-null are comparably virulent following intracranial inoculation of newborn mice (36), even though rsT3D σ 1s-null induces apoptosis less efficiently than

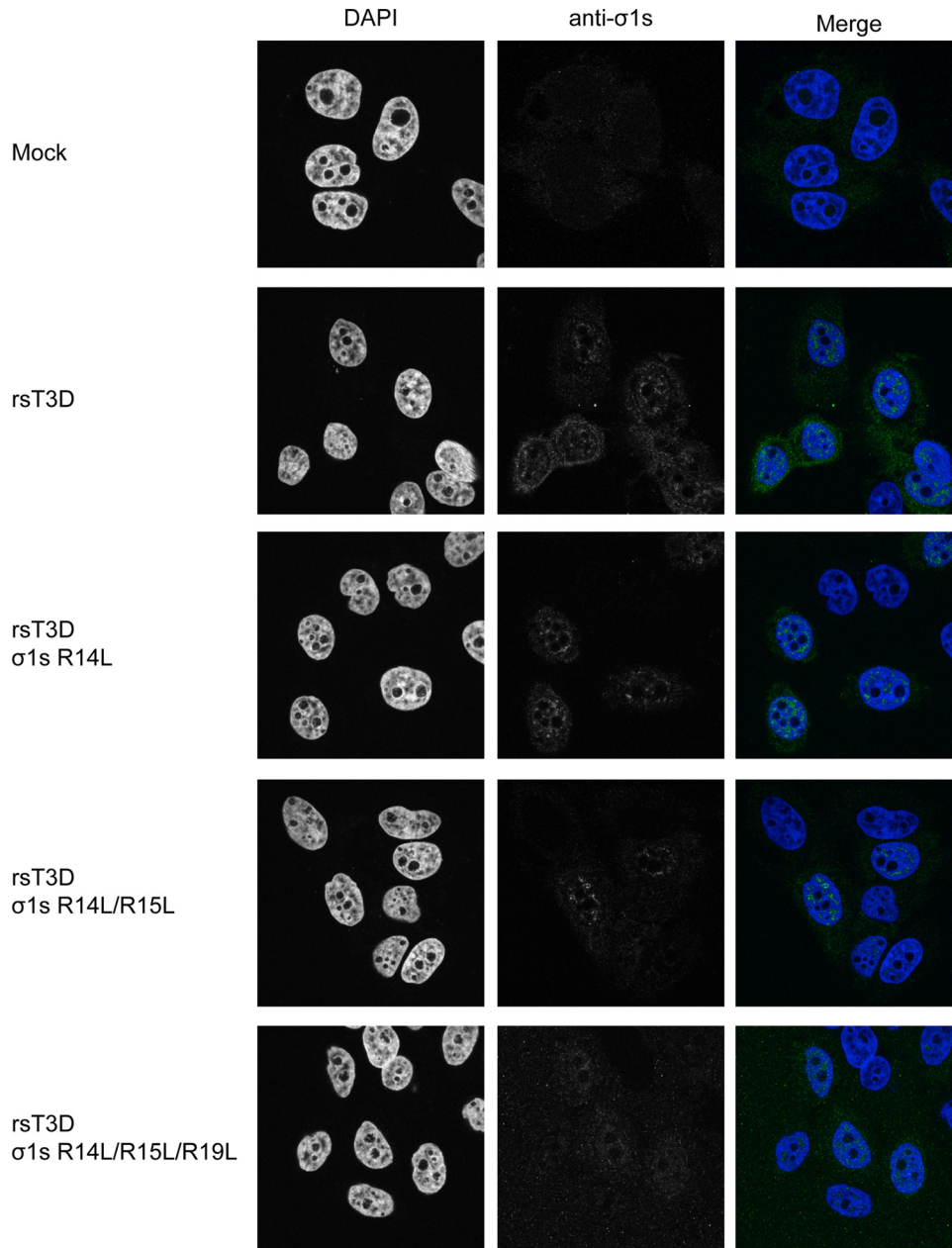


FIG 8 Mutations in the $\sigma 1s$ amino-terminal basic cluster do not affect nuclear translocation of the protein. Cos-7 cells were either mock infected or infected with rsT3D, rsT3D $\sigma 1s$ R14L, rsT3D $\sigma 1s$ R14L/R15L, or rsT3D $\sigma 1s$ R14L/R15L/R19L at an MOI of 10 PFU/cell. Following incubation for 24 h, cells were fixed and stained with a T3D $\sigma 1s$ -specific monoclonal antibody or a reovirus-specific polyclonal antiserum. Nuclei were stained with DAPI.

rsT3D in cultured cells. Unlike most cells in culture, neurons do not divide *in vivo* following completion of a neural developmental program (57). Consequently, $\sigma 1s$ -mediated proapoptotic signals would not be induced in neurons, and apoptosis would result solely from $\sigma 1s$ -independent mechanisms. In keeping with this idea, reovirus can activate proapoptotic networks that function regardless of whether $\sigma 1s$ is expressed. For example, cleavage fragments of outer-capsid protein $\mu 1$ generated during viral disassembly activate intrinsic apoptotic pathways (20, 23). In addition, proinflammatory cytokines secreted in response to reovirus infection may contribute to virus-induced apoptosis by activating death receptors (21, 58–62). Both of these mechanisms are likely

induced by rsT3D and rsT3D $\sigma 1s$ -null in the murine CNS. Although we found that rsT3D infection induces more apoptosis in primary cortical neuron cultures than rsT3D $\sigma 1s$ -null, the difference is not statistically significant. The primary cortical neurons were harvested from mice at E15, which is while neurons are undergoing active cell division (57). Moreover, the cells undergo several rounds of cell division once they are placed in culture (J. L. Konopka-Anstadt and T. S. Dermody, unpublished data). Thus, the modest difference in apoptosis in cultured neurons displayed by rsT3D and rsT3D $\sigma 1s$ -null may reflect the fact that the primary cortical neuron cultures were still dividing.

Apoptosis is initiated during binding and entry of reovirus into

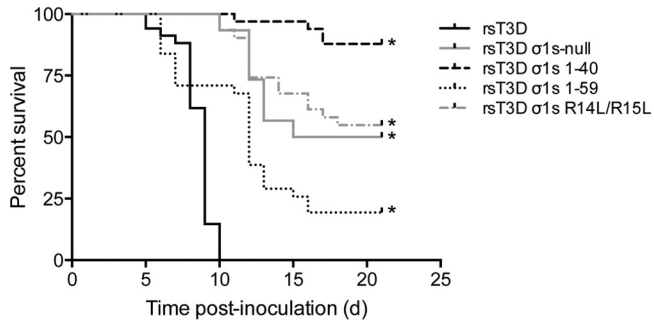


FIG 9 The $\sigma 1s$ amino-terminal basic cluster and amino acids 1 to 59 are required for full reovirus neurovirulence. Newborn C57BL/6 mice were inoculated in the left hind limb with 10^6 PFU of rsT3D, rsT3D $\sigma 1s$ -null, rsT3D $\sigma 1s$ 1–40, rsT3D $\sigma 1s$ 1–59, or rsT3D $\sigma 1s$ R14L/R15L. Mice were monitored for illness for 21 days (d) and euthanized when moribund. *, $P < 0.001$ (as determined by log-rank test in a comparison with rsT3D-infected cells).

host cells. Attachment of $\sigma 1$ to cellular receptors, such as cell surface sialic acid or junctional adhesion molecule A (JAM-A), may provide signals that potentiate apoptosis (63). During reovirus internalization, fragments of outer-capsid protein $\mu 1$ generated by endosomal proteases are delivered into the cytoplasm along with the viral core (20, 64). Once in the cytoplasm, the $\mu 1$ fragments associate with mitochondria, destabilize the mitochondrial membrane, and facilitate cytochrome *c* release and loss of mitochondrial membrane potential (22, 23, 65). Because viral transcription and translation occur subsequent to viral entry, proapoptotic signals are initiated before $\sigma 1s$ is expressed. The $\sigma 1s$ protein may enhance apoptosis by modulating signals initiated by entry-related events. Alternatively, $\sigma 1s$ may activate a different arm of the apoptotic program that boosts the apoptotic capacity of reovirus. Both models are consistent with our finding that rsT3D $\sigma 1s$ -null enhances apoptosis but is not absolutely required for this effect (Fig. 2). It is likely that apoptosis in rsT3D $\sigma 1s$ -null-infected cells results from entry-related proapoptotic signaling. It remains to be determined how signals from $\sigma 1s$ integrate with the activities of capsid components known to induce apoptosis.

One of the hallmarks of *Reoviridae* viruses is that disease develops primarily in neonatal or juvenile hosts (5). At these stages of development, high levels of cell division occur to support rapid growth. If $\sigma 1s$ -dependent cell cycle arrest and apoptosis are triggered in dividing cells, it is possible that the proapoptotic activity of $\sigma 1s$ contributes to the enhanced pathogenesis of reovirus observed in younger hosts. Although rsT3D and rsT3D $\sigma 1s$ -null are comparably virulent following intracranial inoculation, rsT3D $\sigma 1s$ -null is dramatically attenuated relative to rsT3D after hind limb inoculation of newborn mice (36). Attenuation of rsT3D $\sigma 1s$ -null is due to failure of the virus to disseminate systemically via the blood, which impairs viral delivery to the brain and subsequent CNS disease (36). Similarly, a serotype 1 $\sigma 1s$ -null reovirus also fails to spread hematogenously following peroral inoculation (37). We found that mutant viruses that do not induce cell cycle arrest and apoptosis also are attenuated relative to wild-type virus following hind limb inoculation (Fig. 9). These observations raise the possibility that induction of cell cycle arrest and apoptosis following infection at peripheral sites, such as the intestine or hind limb muscle, facilitate hematogenous reovirus dissemination. In at least some circumstances, apoptosis is an immunologically si-

lent process that does not activate immune or inflammatory responses. However, some apoptotic cells secrete a subset of proinflammatory chemokines and cytokines (3) along with soluble factors, such as ATP and UTP, that recruit phagocytes to clear debris from dying cells (2, 4). Following peroral inoculation, reovirus induces apoptosis in intestinal epithelial cells that are taken up by Peyer's patch dendritic cells (66). It is possible that $\sigma 1s$ causes cell cycle arrest and apoptosis in reovirus-infected intestinal epithelial cells and that apoptotic cells filled with progeny virus are engulfed by phagocytic cells, which are in turn responsible for systemic viral dissemination from the site of inoculation.

Reoviruses normally infect their hosts via the intestinal tract, where intestinal epithelial cells undergo continuous replication and shedding. Rapid epithelial cell turnover prevents pathogens from gaining a foothold in the intestine via physiologic turnover of infected cells. Impairing intestinal epithelial cell renewal may slow the process of cell shedding and allow reovirus to persist in the gut of an infected host. Intestinal bacteria, including enteropathogenic and enterohemorrhagic *Escherichia coli*, *Salmonella enterica* serovar Typhi, and *Shigella dysenteriae* encode cyclomodulins that inhibit cell cycle progression (67, 68). Although the function of cyclomodulins has not been defined *in vivo*, these molecules are hypothesized to prevent renewal of the intestinal epithelium to allow bacterial colonization. In the intestine, reovirus antigen is detected in villus epithelial cells and cells at the base of intestinal crypts (69). Stem cells in intestinal crypts are self-renewing and serve as the source of epithelial cells that line the villi. Inhibiting cell cycle progression in crypt cells would slow epithelial cell migration from the crypt to the villus tips and allow reovirus to persist in the intestine. Following peroral inoculation, titers of the serotype 1 $\sigma 1s$ -null virus in the intestine are lower than those produced by wild-type virus (37). By failing to cause cell cycle arrest in intestinal epithelial cells, the $\sigma 1s$ -null virus would not be anticipated to affect the normal turnover of the intestinal lining, which would explain its diminished capacity to infect the intestine.

Reovirus is one of many RNA viruses that modulate cell cycle progression during infection. Like mammalian reovirus, avian reovirus (51), Borna disease virus (70), hepatitis C virus (71), infectious bronchitis virus (44), and respiratory syncytial virus (72) cause cell cycle arrest in G_2 . Other RNA viruses, including coronavirus (73), influenza virus (74), and measles virus (75, 76), arrest the cell cycle in G_1 . Although much is known about the relationship between DNA viruses and the cell cycle, little is understood about how or why RNA viruses dysregulate this vital

TABLE 1 Survival statistics following intramuscular inoculation^a

Virus strain	No. of animals inoculated	No. of events ^b	% survival	Median survival time (days)
rsT3D	34	34	0	9
rsT3D $\sigma 1s$ -null	30	15	50	18
rsT3D $\sigma 1s$ 1–40	33	4	88	>21
rsT3D $\sigma 1s$ 1–59	31	25	19	12
rsT3D $\sigma 1s$ R14L/R15L	31	14	55	>21

^a Newborn C57BL/6 mice were inoculated intramuscularly in the left hind limb with 10^6 PFU of the indicated strains. Mice were monitored for signs of disease for 21 days postinoculation and euthanized when moribund.

^b Number of mice that did not survive the 21-day observation period.

cellular process. DNA viruses, such as adenovirus or papillomavirus, drive the cell into S phase to create a suitable environment for viral DNA replication (77). Perhaps G₂ is the optimal cell cycle stage for reovirus replication. It is noteworthy that the $\sigma 1s$ protein is not required for reovirus replication in cultured cells (32, 36, 37). However, these studies were performed using transformed cells, including HeLa, L929, and MDCK cells. Transformed cells are more metabolically active than the majority of cells *in vivo*. Because they cycle rapidly, transformed cells enter each stage of the cell cycle more frequently than nontransformed cells. Thus, any benefit gained by halting cell cycle progression in transformed cells may not provide a $\sigma 1s$ -expressing virus with a replication advantage. Because transformed cells divide rapidly, it is possible that they are more susceptible to $\sigma 1s$ -mediated apoptosis. Based on an enhanced capacity to infect and kill cancer cells, reovirus is currently being evaluated in clinical trials as an oncolytic adjunct to conventional chemotherapy (78, 79). If $\sigma 1s$ -mediated effects on cell cycle control are more evident in proliferating cells, then $\sigma 1s$ -dependent cell cycle arrest and apoptosis may be important mechanisms underlying reovirus oncolysis.

The $\sigma 1s$ protein is one of many viral nonstructural proteins that induce cell cycle arrest and apoptosis. Adenovirus E4orf4 (80, 81), avian reovirus p17 (51), and HIV Vpr (82–86) cause both effects, whereas other viral nonstructural proteins, such as influenza virus PB1-F2 (87), directly induce apoptosis. Apoptotic cell death is an important component of the host response to viral infection. Apoptosis limits viral replication in infected cells and alerts adaptive immune responses to the presence of an invading pathogen. Consequently, viruses use multiple strategies to limit apoptosis, which allows the virus to evade immune detection. It is not clear why viruses encode proteins that actively promote a cellular process specifically designed to combat viral infection. Determining how $\sigma 1s$ modulates host cell cycle progression and apoptosis will enhance an understanding of the molecular and cellular basis of reovirus cell cycle arrest, apoptosis, and dissemination and may provide new knowledge about how and why viral nonstructural proteins from numerous viruses promote these effects. Given the likelihood of significant interplay between $\sigma 1s$ and cell cycle control pathways, enhanced knowledge of $\sigma 1s$ function also may lead to new insights into these highly regulated, interrelated processes that play fundamental roles in development, immunity, and cancer.

ACKNOWLEDGMENTS

The flow cytometry experiments were performed in the Vanderbilt Cytometry Shared Resource. David Cortez (Vanderbilt University) provided HCT-116 cells. We thank Dan Voth for assistance with confocal microscopy.

This work was supported by Public Health Service awards T32 CA09385 (K.W.B.), F32 AI075776 (K.W.B.), K22 AI94079 (K.W.B.), P20 GM103625 (K.W.B.), T32 CA09385 (J.L.K.-A.), F32 AI081486 (J.L.K.-A.), and R37 AI38296 (T.S.D.) and the Elizabeth B. Lamb Center for Pediatric Research. Additional support was provided by Public Health Service awards CA68485 for the Vanderbilt-Ingram Cancer Center and DK20593 for the Vanderbilt Diabetes Research and Training Center.

REFERENCES

- Roulston A, Marcellus RC, Branton PE. 1999. Viruses and apoptosis. *Annu. Rev. Microbiol.* 53:577–628.
- Chekeni FB, Elliott MR, Sandilos JK, Walk SF, Kinchen JM, Lazarowski ER, Armstrong AJ, Penuela S, Laird DW, Salvesen GS, Isakson BE, Bayliss DA, Ravichandran KS. 2010. Pannexin 1 channels mediate ‘find-me’ signal release and membrane permeability during apoptosis. *Nature* 467:863–867.
- Cullen SP, Henry CM, Kearney CJ, Logue SE, Feoktistova M, Tynan GA, Lavelle EC, Leverkus M, Martin SJ. 2013. Fas/CD95-induced chemokines can serve as “find-me” signals for apoptotic cells. *Mol. Cell* 49:1034–1048.
- Elliott MR, Chekeni FB, Trampont PC, Lazarowski ER, Kadl A, Walk SF, Park D, Woodson RI, Ostankovich M, Sharma P, Lysiak JJ, Harden TK, Leitinger N, Ravichandran KS. 2009. Nucleotides released by apoptotic cells act as a find-me signal to promote phagocytic clearance. *Nature* 461:282–286.
- Dermody TS, Parker J, Sherry B. 2013. Orthoreovirus. In Knipe DM, Howley PM, Cohen JL, Griffin DE, Lamb RA, Martin MA, Racaniello VR, Roizman B (ed), *Fields virology*, 6th ed, vol 2, p 1304–1346. Lippincott Williams & Wilkins, Philadelphia, PA.
- Dichter MA, Weiner HL. 1984. Infection of neuronal cell cultures with reovirus mimics in vitro patterns of neurotropism. *Ann. Neurol.* 16:603–610.
- Tardieu M, Weiner HL. 1982. Viral receptors on isolated murine and human ependymal cells. *Science* 215:419–421.
- Tyler KL, McPhee DA, Fields BN. 1986. Distinct pathways of viral spread in the host determined by reovirus S1 gene segment. *Science* 233:770–774.
- Tyler KL, Squier MKT, Brown AL, Pike B, Willis D, Oberhaus SM, Dermody TS, Cohen JJ. 1996. Linkage between reovirus-induced apoptosis and inhibition of cellular DNA synthesis: role of the S1 and M2 genes. *J. Virol.* 70:7984–7991.
- Morrison LA, Sidman RL, Fields BN. 1991. Direct spread of reovirus from the intestinal lumen to the central nervous system through vagal autonomic nerve fibers. *Proc. Natl. Acad. Sci. U. S. A.* 88:3852–3856.
- Weiner HL, Drayna D, Averill DR, Jr, Fields BN. 1977. Molecular basis of reovirus virulence: role of the S1 gene. *Proc. Natl. Acad. Sci. U. S. A.* 74:5744–5748.
- Weiner HL, Powers ML, Fields BN. 1980. Absolute linkage of virulence and central nervous system tropism of reoviruses to viral hemagglutinin. *J. Infect. Dis.* 141:609–616.
- Tyler KL, Squier MK, Rodgers SE, Schneider SE, Oberhaus SM, Grdina TA, Cohen JJ, Dermody TS. 1995. Differences in the capacity of reovirus strains to induce apoptosis are determined by the viral attachment protein $\sigma 1$. *J. Virol.* 69:6972–6979.
- McCrae JA, Joklik WK. 1978. The nature of the polypeptide encoded by each of the ten double-stranded RNA segments of reovirus type 3. *Virology* 89:578–593.
- Mustoe TA, Ramig RF, Sharpe AH, Fields BN. 1978. Genetics of reovirus: identification of the dsRNA segments encoding the polypeptides of the μ and σ size classes. *Virology* 89:594–604.
- Sarkar G, Pelletier J, Bassel-Duby R, Jayasuriya A, Fields BN, Sonenberg N. 1985. Identification of a new polypeptide coded by reovirus gene S1. *J. Virol.* 54:720–725.
- Weiner HL, Ault KA, Fields BN. 1980. Interaction of reovirus with cell surface receptors. I. Murine and human lymphocytes have a receptor for the hemagglutinin of reovirus type 3. *J. Immunol.* 124:2143–2148.
- Danthi P, Hansberger MW, Campbell JA, Forrest JC, Dermody TS. 2006. JAM-A-independent, antibody-mediated uptake of reovirus into cells leads to apoptosis. *J. Virol.* 80:1261–1270.
- Coffey CM, Sheh A, Kim IS, Chandran K, Nibert ML, Parker JS. 2006. Reovirus outer capsid protein $\mu 1$ induces apoptosis and associates with lipid droplets, endoplasmic reticulum, and mitochondria. *J. Virol.* 80:8422–8438.
- Danthi P, Coffey CM, Parker JS, Abel TW, Dermody TS. 2008. Independent regulation of reovirus membrane penetration and apoptosis by the $\mu 1$ ϕ domain. *PLoS Pathog.* 4:e1000248. doi:10.1371/journal.ppat.1000248.
- Danthi P, Pruijssers AJ, Berger AK, Holm GH, Zinkel SS, Dermody TS. 2010. Bid regulates the pathogenesis of neurotropic reovirus. *PLoS Pathog.* 6:e1000980. doi:10.1371/journal.ppat.1000980.
- Kim JW, Lyi SM, Parrish CR, Parker JS. 2011. A proapoptotic peptide derived from reovirus outer capsid protein $\mu 1$ has membrane-destabilizing activity. *J. Virol.* 85:1507–1516.
- Wisniewski ML, Werner BG, Hom LG, Anguish LJ, Coffey CM, Parker JS. 2011. Reovirus infection or ectopic expression of outer capsid protein $\mu 1$ induces apoptosis independently of the cellular proapoptotic proteins Bax and Bak. *J. Virol.* 85:296–304.

24. Cashdollar LW, Chmelo RA, Wiener JR, Joklik WK. 1985. Sequences of the S1 genes of the three serotypes of reovirus. *Proc. Natl. Acad. Sci. U. S. A.* 82:24–28.
25. Ernst H, Shatkin AJ. 1985. Reovirus hemagglutinin mRNA codes for two polypeptides in overlapping reading frames. *Proc. Natl. Acad. Sci. U. S. A.* 82:48–52.
26. Cenatiempo Y, Twardowski T, Shoeman R, Ernst H, Brot N, Weissbach H, Shatkin AJ. 1984. Two initiation sites detected in the small s1 species of reovirus mRNA by dipeptide synthesis in vitro. *Proc. Natl. Acad. Sci. U. S. A.* 81:1084–1088.
27. Dermody TS, Nibert ML, Bassel-Duby R, Fields BN. 1990. Sequence diversity in S1 genes and S1 translation products of 11 serotype 3 reovirus strains. *J. Virol.* 64:4842–4850.
28. Hoyt CC, Bouchard RJ, Tyler KL. 2004. Novel nuclear herniations induced by nuclear localization of a viral protein. *J. Virol.* 78:6360–6369.
29. Poggioli GJ, Dermody TS, Tyler KL. 2001. Reovirus-induced σ 1s-dependent G₂/M cell cycle arrest results from inhibition of p34cdc2. *J. Virol.* 75:7429–7434.
30. Poggioli GJ, Keefer CJ, Connolly JL, Dermody TS, Tyler KL. 2000. Reovirus-induced G₂/M cell cycle arrest requires σ 1s and occurs in the absence of apoptosis. *J. Virol.* 74:9562–9570.
31. Hoyt CC, Richardson-Burns SM, Goody RJ, Robinson BA, Debiasi RL, Tyler KL. 2005. Nonstructural protein σ 1s is a determinant of reovirus virulence and influences the kinetics and severity of apoptosis induction in the heart and central nervous system. *J. Virol.* 79:2743–2753.
32. Rodgers SE, Connolly JL, Chappell JD, Dermody TS. 1998. Reovirus growth in cell culture does not require the full complement of viral proteins: identification of a σ 1s-null mutant. *J. Virol.* 72:8597–8604.
33. Chappell JD, Gunn VL, Wetzel JD, Baer GS, Dermody TS. 1997. Mutations in type 3 reovirus that determine binding to sialic acid are contained in the fibrous tail domain of viral attachment protein σ 1. *J. Virol.* 71:1834–1841.
34. Connolly JL, Barton ES, Dermody TS. 2001. Reovirus binding to cell surface sialic acid potentiates virus-induced apoptosis. *J. Virol.* 75:4029–4039.
35. Barton ES, Youree BE, Ebert DH, Forrest JC, Connolly JL, Valyi-Nagy T, Washington K, Wetzel JD, Dermody TS. 2003. Utilization of sialic acid as a coreceptor is required for reovirus-induced biliary disease. *J. Clin. Invest.* 111:1823–1833.
36. Boehme KW, Frierson JM, Konopka JL, Kobayashi T, Dermody TS. 2011. The reovirus σ 1s protein is a determinant of hematogenous but not neural virus dissemination in mice. *J. Virol.* 85:11781–11790.
37. Boehme KW, Guglielmi KM, Dermody TS. 2009. Reovirus nonstructural protein σ 1s is required for establishment of viremia and systemic dissemination. *Proc. Natl. Acad. Sci. U. S. A.* 106:19986–19991.
38. Antar AAR, Konopka JL, Campbell JA, Henry RA, Perdigoto AL, Carter BD, Pozzi A, Abel TW, Dermody TS. 2009. Junctional adhesion molecule-A is required for hematogenous dissemination of reovirus. *Cell Host Microbe* 5:59–71.
39. Kobayashi T, Antar AAR, Boehme KW, Danthi P, Eby EA, Guglielmi KM, Holm GH, Johnson EM, Maginnis MS, Naik S, Skelton WB, Wetzel JD, Wilson GJ, Chappell JD, Dermody TS. 2007. A plasmid-based reverse genetics system for animal double-stranded RNA viruses. *Cell Host Microbe* 1:147–157.
40. Virgin HW, Bassel-Duby IVR, Fields BN, Tyler KL. 1988. Antibody protects against lethal infection with the neurally spreading reovirus type 3 (Dearing). *J. Virol.* 62:4594–4604.
41. Furlong DB, Nibert ML, Fields BN. 1988. Sigma 1 protein of mammalian reoviruses extends from the surfaces of viral particles. *J. Virol.* 62:246–256.
42. Smith RE, Zweerink HJ, Joklik WK. 1969. Polypeptide components of virions, top component and cores of reovirus type 3. *Virology* 39:791–810.
43. Yao K, Vakharia VN. 1998. Generation of infectious pancreatic necrosis virus from cloned cDNA. *J. Virol.* 72:8913–8920.
44. Dove B, Brooks G, Bicknell K, Wurm T, Hiscox JA. 2006. Cell cycle perturbations induced by infection with the coronavirus infectious bronchitis virus and their effect on virus replication. *J. Virol.* 80:4147–4156.
45. Bodkin DK, Fields BN. 1989. Growth and survival of reovirus in intestinal tissue: role of the L2 and S1 genes. *J. Virol.* 63:1188–1193.
46. Bodkin DK, Nibert ML, Fields BN. 1989. Proteolytic digestion of reovirus in the intestinal lumens of neonatal mice. *J. Virol.* 63:4676–4681.
47. Nibert ML, Chappell JD, Dermody TS. 1995. Infectious subvirion particles of reovirus type 3 Dearing exhibit a loss in infectivity and contain a cleaved σ 1 protein. *J. Virol.* 69:5057–5067.
48. Sperka T, Wang J, Rudolph KL. 2012. DNA damage checkpoints in stem cells, ageing and cancer. *Nat. Rev. Mol. Cell Biol.* 13:579–590.
49. Turnell AS, Grand RJ. 2012. DNA viruses and the cellular DNA-damage response. *J. Gen. Virol.* 93:2076–2097.
50. Baer A, Austin D, Narayanan A, Popova T, Kainulainen M, Bailey C, Kashanchi F, Weber F, Kehm-Hall K. 2012. Induction of DNA damage signaling upon Rift Valley fever virus infection results in cell cycle arrest and increased viral replication. *J. Biol. Chem.* 287:7399–7410.
51. Chulu JL, Huang WR, Wang L, Shih WL, Liu HJ. 2010. Avian reovirus nonstructural protein p17-induced G₂/M cell cycle arrest and host cellular protein translation shutoff involve activation of p53-dependent pathways. *J. Virol.* 84:7683–7694.
52. Kornitzer D, Sharf R, Kleinberger T. 2001. Adenovirus E4orf4 protein induces PP2A-dependent growth arrest in *Saccharomyces cerevisiae* and interacts with the anaphase-promoting complex/cyclosome. *J. Cell Biol.* 154:331–344.
53. Kim S, Park SY, Yong H, Famulski JK, Chae S, Lee JH, Kang CM, Saya H, Chan GK, Cho H. 2008. HBV X protein targets hBubR1, which induces dysregulation of the mitotic checkpoint. *Oncogene* 27:3457–3464.
54. Heilman DW, Green MR, Teodoro JG. 2005. The anaphase promoting complex: a critical target for viral proteins and anti-cancer drugs. *Cell Cycle* 4:560–563.
55. Liu Y, Rusinol A, Sinensky M, Wang Y, Zou Y. 2006. DNA damage responses in progeroid syndromes arise from defective maturation of prelamin A. *J. Cell Sci.* 119:4644–4649.
56. Manju K, Muralikrishna B, Parnaik VK. 2006. Expression of disease-causing lamin A mutants impairs the formation of DNA repair foci. *J. Cell Sci.* 119:2704–2714.
57. Dehay C, Kennedy H. 2007. Cell-cycle control and cortical development. *Nat. Rev. Neurosci.* 8:438–450.
58. Clarke P, Beckham JD, Leser JS, Hoyt CC, Tyler KL. 2009. Fas-mediated apoptotic signaling in the mouse brain following reovirus infection. *J. Virol.* 83:6161–6170.
59. Clarke P, Meintzer SM, Gibson S, Widmann C, Garrington TP, Johnson GL, Tyler KL. 2000. Reovirus-induced apoptosis is mediated by TRAIL. *J. Virol.* 74:8135–8139.
60. Clarke P, Meintzer SM, Spalding AC, Johnson GL, Tyler KL. 2001. Caspase 8-dependent sensitization of cancer cells to TRAIL-induced apoptosis following reovirus-infection. *Oncogene* 20:6910–6919.
61. Kominsky DJ, Bickel RJ, Tyler KL. 2002. Reovirus-induced apoptosis requires both death receptor- and mitochondrial-mediated caspase-dependent pathways of cell death. *Cell Death Differ.* 9:926–933.
62. Richardson-Burns SM, Kominsky DJ, Tyler KL. 2002. Reovirus-induced neuronal apoptosis is mediated by caspase 3 and is associated with the activation of death receptors. *J. Neurovirol.* 8:365–380.
63. Barton ES, Forrest JC, Connolly JL, Chappell JD, Liu Y, Schnell F, Nusrat A, Parkos CA, Dermody TS. 2001. Junctional adhesion molecule is a receptor for reovirus. *Cell* 104:441–451.
64. Danthi P, Kobayashi T, Holm GH, Hansberger MW, Abel TW, Dermody TS. 2008. Reovirus apoptosis and virulence are regulated by host cell membrane-penetration efficiency. *J. Virol.* 82:161–172.
65. Kaufer S, Coffey CM, Parker JS. 2012. The cellular chaperone hsc70 is specifically recruited to reovirus viral factories independently of its chaperone function. *J. Virol.* 86:1079–1089.
66. Fleeton M, Contractor N, Leon F, Wetzel JD, Dermody TS, Kelsall B. 2004. Peyer's patch dendritic cells process viral antigen from apoptotic epithelial cells in the intestine of reovirus-infected mice. *J. Exp. Med.* 200:235–245.
67. Jubelin G, Chavez CV, Taieb F, Banfield MJ, Samba-Louaka A, Nobe R, Nougayrede JP, Zumbihl R, Givaudan A, Escoubas JM, Oswald E. 2009. Cycle inhibiting factors (CIFs) are a growing family of functional cyclomodulins present in invertebrate and mammal bacterial pathogens. *PLoS One* 4:e4855. doi:10.1371/journal.pone.0004855.
68. Oswald E, Nougayrede JP, Taieb F, Sugai M. 2005. Bacterial toxins that modulate host cell-cycle progression. *Curr. Opin. Microbiol.* 8:83–91.
69. Rubin DH, Kornstein MJ, Anderson AO. 1985. Reovirus serotype 1 intestinal infection: a novel replicative cycle with ileal disease. *J. Virol.* 53:391–398.
70. Planz O, Pleschka S, Oesterle K, Berberich-Siebelt F, Ehrhardt C, Stitz

- L, Ludwig S. 2003. Borna disease virus nucleoprotein interacts with the CDC2-cyclin B1 complex. *J. Virol.* 77:11186–11192.
71. Kannan RP, Hensley LL, Evers LE, Lemon SM, McGovern DR. 2011. Hepatitis C virus infection causes cell cycle arrest at the level of initiation of mitosis. *J. Virol.* 85:7989–8001.
 72. Bian T, Gibbs JD, Orvell C, Imani F. 2012. Respiratory syncytial virus matrix protein induces lung epithelial cell cycle arrest through a p53 dependent pathway. *PLoS One* 7:e38052. doi:10.1371/journal.pone.0038052.
 73. Chen CJ, Makino S. 2004. Murine coronavirus replication induces cell cycle arrest in G₀/G₁ phase. *J. Virol.* 78:5658–5669.
 74. He Y, Xu K, Keiner B, Zhou J, Czudai V, Li T, Chen Z, Liu J, Klenk HD, Shu YL, Sun B. 2010. Influenza A virus replication induces cell cycle arrest in G₀/G₁ phase. *J. Virol.* 84:12832–12840.
 75. McChesney MB, Altman A, Oldstone MB. 1988. Suppression of T lymphocyte function by measles virus is due to cell cycle arrest in G₁. *J. Immunol.* 140:1269–1273.
 76. McChesney MB, Kehrl JH, Valsamakis A, Fauci AS, Oldstone MB. 1987. Measles virus infection of B lymphocytes permits cellular activation but blocks progression through the cell cycle. *J. Virol.* 61:3441–3447.
 77. Dyson N, Howley PM, Munger K, Harlow E. 1989. The human papilloma virus-16 E7 oncoprotein is able to bind to the retinoblastoma gene product. *Science* 243:934–937.
 78. Adair RA, Roulstone V, Scott KJ, Morgan R, Nuovo GJ, Fuller M, Beirne D, West EJ, Jennings VA, Rose A, Kyula J, Fraser S, Dave R, Anthony DA, Merrick A, Prestwich R, Aldouri A, Donnelly O, Pandha H, Coffey M, Selby P, Vile R, Toogood G, Harrington K, Melcher AA. 2012. Cell carriage, delivery, and selective replication of an oncolytic virus in tumor in patients. *Sci. Transl. Med.* 4:138ra177.
 79. Karapanagiotou EM, Roulstone V, Twigger K, Ball M, Tanay M, Nutting C, Newbold K, Gore ME, Larkin J, Syrigos KN, Coffey M, Thompson B, Mettinger K, Vile RG, Pandha HS, Hall GD, Melcher AA, Chester J, Harrington KJ. 2012. Phase I/II trial of carboplatin and paclitaxel chemotherapy in combination with intravenous oncolytic reovirus in patients with advanced malignancies. *Clin. Cancer Res.* 18:2080–2089.
 80. Lavoie JN, Nguyen M, Marcellus RC, Branton PE, Shore GC. 1998. E4orf4, a novel adenovirus death factor that induces p53-independent apoptosis by a pathway that is not inhibited by zVAD-fmk. *J. Cell Biol.* 140:637–645.
 81. Marcellus RC, Lavoie JN, Boivin D, Shore GC, Ketner G, Branton PE. 1998. The early region 4 orf4 protein of human adenovirus type 5 induces p53-independent cell death by apoptosis. *J. Virol.* 72:7144–7153.
 82. Bartz SR, Rogel ME, Emerman M. 1996. Human immunodeficiency virus type 1 cell cycle control: Vpr is cytostatic and mediates G₂ accumulation by a mechanism which differs from DNA damage checkpoint control. *J. Virol.* 70:2324–2331.
 83. He J, Choe S, Walker R, Di Marzio P, Morgan DO, Landau NR. 1995. Human immunodeficiency virus type 1 viral protein R (Vpr) arrests cells in the G₂ phase of the cell cycle by inhibiting p34cdc2 activity. *J. Virol.* 69:6705–6711.
 84. Jowett JB, Planelles V, Poon B, Shah NP, Chen ML, Chen IS. 1995. The human immunodeficiency virus type 1 *vpr* gene arrests infected T cells in the G₂ + M phase of the cell cycle. *J. Virol.* 69:6304–6313.
 85. Re F, Braaten D, Franke EK, Luban J. 1995. Human immunodeficiency virus type 1 Vpr arrests the cell cycle in G₂ by inhibiting the activation of p34cdc2-cyclin B. *J. Virol.* 69:6859–6864.
 86. Rogel ME, Wu LI, Emerman M. 1995. The human immunodeficiency virus type 1 *vpr* gene prevents cell proliferation during chronic infection. *J. Virol.* 69:882–888.
 87. Zamarin D, Garcia-Sastre A, Xiao X, Wang R, Palese P. 2005. Influenza virus PB1-F2 protein induces cell death through mitochondrial ANT3 and VDAC1. *PLoS Pathog.* 1:e4. doi:10.1371/journal.ppat.0010004.